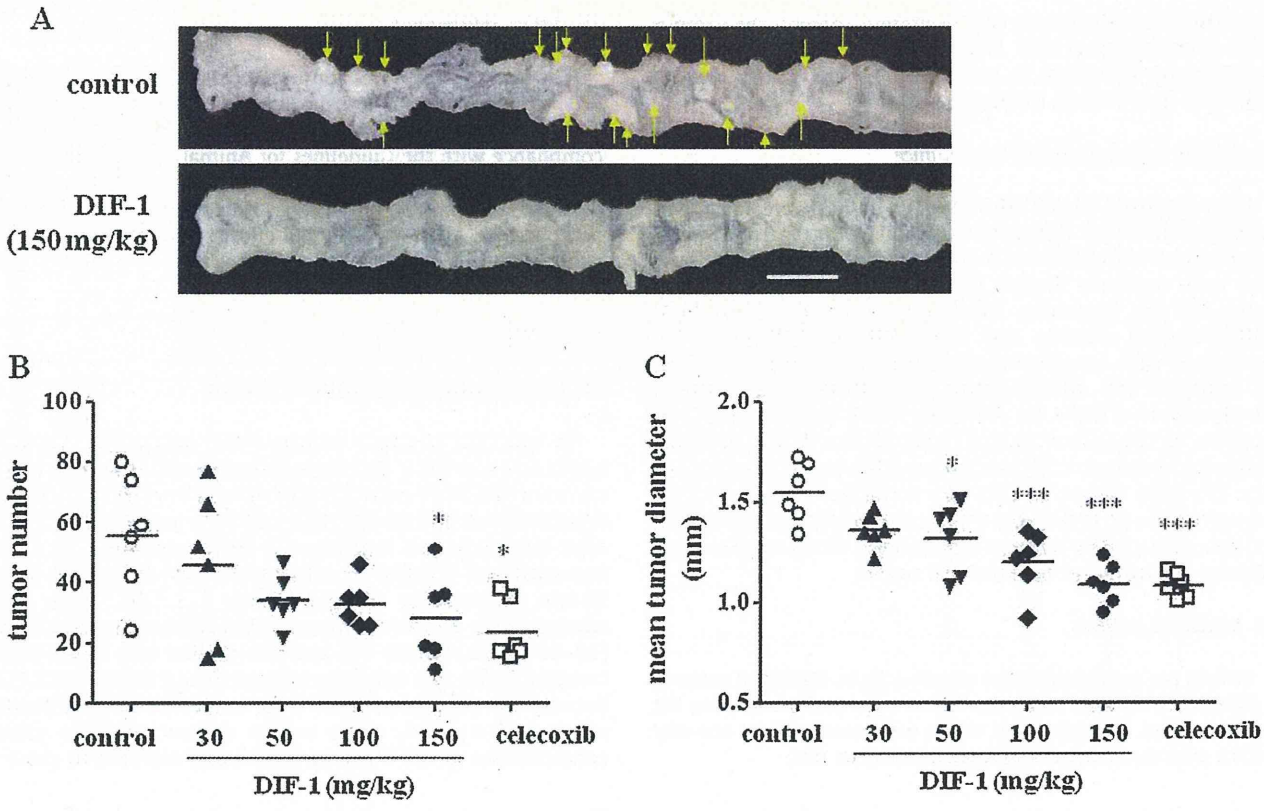

Fig. 2. Effect of DIF-1 on intestinal tumors induced by $KBrO_3$ in *Mutyh*$^{-/-}$ mice.
A. Proximal region of the small intestines. Scale bar indicates 1 cm. Arrows indicate tumors with a >2.5 mm diameter. B. Tumor numbers are plotted for each mouse. Horizontal bars indicate the means of each group ($n = 6$). C. Mean tumor diameters are plotted for each mouse. Horizontal bars indicate the means of each group ($n = 6$). $^{*}P < 0.05$ vs. control, $^{***}P < 0.001$ (one-way ANOVA with Dunnett's multiple comparison test).

antiproliferative effect *in vivo*. Therefore, we used oral administration for the following experiments.

3.2. Effect of DIF-1 on oxidative stress-induced tumors in *Mutyh*$^{-/-}$ mice

To evaluate the anti-tumor effect of DIF-1 *in vivo*, we first used mice deficient for MUTYH, an enzyme that prevents formation of oxidative stress-induced DNA lesions. Studies have shown that MUTYH deficiency might be involved in the development of colorectal adenoma and carcinoma in humans [28–30]. As we reported previously [31], the occurrence of carcinomas in the small intestine was dramatically increased by oxidative stress in *Mutyh*$^{-/-}$ mice. Twelve weeks of treatment with 0.2% $KBrO_3$, a strong oxidant, followed by vehicle treatment for 4 weeks induced numerous intestinal tumors (55.7 ± 8.4, $n = 6$) in *Mutyh*$^{-/-}$ mice, whereas only a small number of tumors were formed in wild-type mice (1.2 ± 0.5, $n = 6$).

We administered DIF-1 or celecoxib to *Mutyh*$^{-/-}$ mice for 4 weeks to examine the effects of these compounds. We used celecoxib for reference because it has been used for the treatment of FAP patients [34]. DIF-1 treatment (10–150 mg/kg/day for 4 weeks) markedly reduced the number and size of intestinal tumors in a dose-dependent manner (Fig. 2A–C). The effectiveness of DIF-1 appeared to be comparable with that of celecoxib, because the same doses (150 mg/kg) of these compounds showed similar effects.

Next, we carried out Western blot analyses of tumor samples obtained from vehicle- or DIF-1 (150 mg/kg)-treated mice. Because DIF-1 activates GSK-3β by dephosphorylation of Ser^9 in cultured cells [22,23,25], we analyzed the effect of DIF-1 on the phosphorylation status of GSK-3β Ser^9 in the intestines. As shown in Fig. 3A, DIF-1 significantly decreased the phosphorylation level of GSK-3β Ser^9, suggesting that DIF-1 also activated GSK-3β *in vivo*. Furthermore, DIF-1 markedly decreased the protein expression levels of Egr-1, TCF7L2 and cyclin D1, although β-catenin levels were unaltered (Fig. 3B). These results suggested that DIF-1 inhibited tumor growth in *Mutyh*$^{-/-}$ mice by GSK-3β-mediated suppression of cyclin D1 expression and Egr-1-mediated suppression of TCF7L2 expression.

To examine whether long-term treatment with DIF-1 shows adverse effect on the general condition, we measured their body weight and peripheral blood cell counts, as well as observing their appearance and activity. Red blood cell (RBC) numbers and hemoglobin (Hb) concentrations were significantly lower in *Mutyh*$^{-/-}$ mice compared with those in wild-type mice (Table 1). *Mutyh*$^{-/-}$ mice may have suffered from anemia caused by intestinal bleeding due to developed tumors, because excrement from *Mutyh*$^{-/-}$ mice was strongly positive (+++) for occult blood, whereas excrement from wild-type mice was negative (data not shown). There were no significant differences in white blood cell (WBC) or platelet numbers and changes in body weight (ΔBW) between *Mutyh*$^{-/-}$ mice and wild-type mice. Administration of DIF-1 or celecoxib did not affect the appearance, activity, WBC and platelet numbers, or ΔBW of the mice. However, DIF-1 and celecoxib significantly increased RBC counts and Hb levels, suggesting that these compounds prevent bleeding from the intestinal mucosa by reducing size and number of tumors (Table 1).

Please cite this article in press as: Takahashi-Yanaga F, et al. DIF-1 inhibits tumor growth *in vivo* reducing phosphorylation of GSK-3β and expressions of cyclin D1 and TCF7L2 in cancer model mice. Biochem Pharmacol (2014), http://dx.doi.org/10.1016/j.bcp.2014.03.006

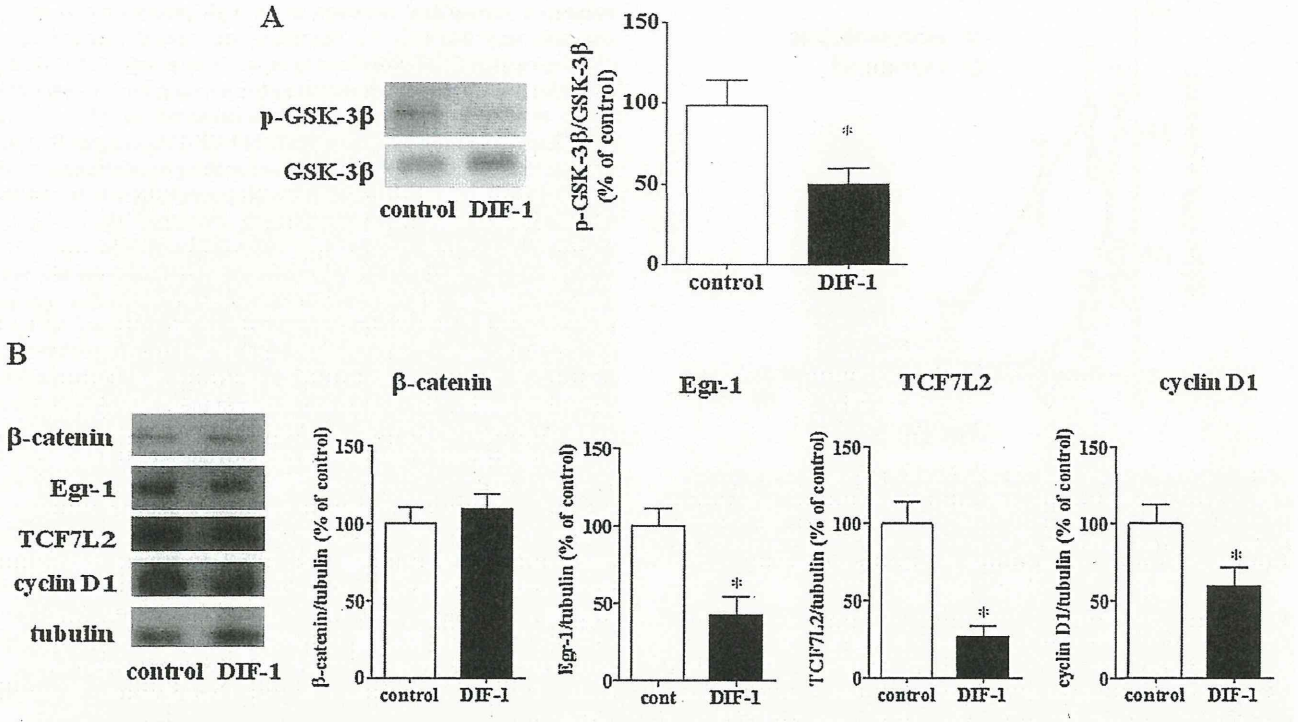

Fig. 3. Western blot analyses of proteins extracted from *Mutyh*$^{-/-}$ mouse small intestines.
Protein samples prepared from the small intestines of vehicle- and DIF-1 (150 mg/kg)-treated mice were analyzed by Western blotting. A. GSK-3β phosphorylation levels. Protein samples were subjected to Western blotting to analyze phosphorylation of GSK-3β Ser^{9} using an anti-phospho-GSK-3β antibody. After stripping, the membranes were reprobed with an anti-GSK-3β antibody. Band densities are shown as percentages of the controls. Values are the means ± s.e.m. ($n = 6$). *$P < 0.05$ vs. control (Student's *t*-test). p-GSK-3β, phospho-GSK-3β. B. Expression levels of β-catenin, Egr-1, TCF7L2, and cyclin D1. Band densities were quantified and normalized to those of tubulin. Values are the means ± s.e.m. ($n = 6$). *$P < 0.05$ vs. control (Student's *t*-test).

3.3. Effect of DIF-1 on human cancer xenografts

Our experiments using *Mutyh*$^{-/-}$ mice showed that DIF-1 inhibited intestinal tumor growth. However, it appeared possible that DIF-1 administered into the digestive tract directly acted on the intestinal mucosa without absorption into systemic circulation. Therefore, we investigated whether orally administered DIF-1 could show an anti-tumor effect on tumors growing in a region distant from the digestive tract. For this purpose, we employed nude mice xenografted with two different cell species of human cancer: HCT-116-xenografted mice to examine the effect of DIF-1 on colon cancer *in vivo* and HeLa-xenografted mice to confirm the effect of DIF-1 in a different cancer. One reason that we chose these two cancer cell species was that the β-catenin destruction mechanism is mutated in HCT-116 but it is intact in HeLa cells. We first treated these xenografted mice with orally administered DIF-1 (150 mg/kg every 24 h) that was suspended in 0.25% methylcellulose (the same solvent used in Mutyh$^{-/-}$ mice experiments). However, DIF-1 failed to show a significant effect on tumor xenografts (data not shown). We considered that this

Table 1
Effects of DIF-1 on blood cell counts and body weight.

		WBC (×10^2 cells/μL)	RBC (×10^4 cells/μL)	Hb (g/dL)	Plt (×10^4 cells/μL)	ΔBW (g)
Wild-type						
Vehicle		58.0 ± 5.7	923.3 ± 16.3	12.2 ± 0.38	52.7 ± 5.5	3.26 ± 0.77
Mutyh$^{-/-}$						
Vehicle		54.6 ± 6.1	615.7 ± 66.4**	10.0 ± 0.93*	64.7 ± 9.5	1.75 ± 0.36
DIF-1	mg/kg					
	10	50.5 ± 6.6	678.8 ± 60.0**	10.6 ± 0.38	65.0 ± 7.9	1.85 ± 0.53
	30	43.7 ± 7.2	682.3 ± 67.0**	11.0 ± 0.69	74.3 ± 5.3	1.87 ± 0.36
	100	65.2 ± 13.1	752.0 ± 34.7	11.6 ± 0.40	58.4 ± 3.9	1.93 ± 0.50
	150	55.9 ± 4.1	787.3 ± 37.7	11.7 ± 0.41	73.0 ± 7.0	2.16 ± 0.66
Celecoxib	mg/kg					
	150	53.5 ± 12.7	828.3 ± 29.1	11.6 ± 0.38	64.1 ± 6.6	2.51 ± 0.53

DIF-1, celecoxib or the vehicle (methylcellulose) was orally administered to mice for 4 weeks. Data represent the means ± s.e.m. Statistical significance was determined by one-way ANOVA with Dunnett's multiple comparison test. $N = 6$ for each group. WBCs, white blood cells; RBCs, red blood cells; Hb, hemoglobin; Plt, platelets; ΔBW, body weight change from 12 to 16 weeks.
* $P < 0.05$ vs. vehicle-treated wild-type mice.
** $P < 0.01$ vs. vehicle-treated wild-type mice.

Please cite this article in press as: Takahashi-Yanaga F, et al. DIF-1 inhibits tumor growth *in vivo* reducing phosphorylation of GSK-3β and expressions of cyclin D1 and TCF7L2 in cancer model mice. Biochem Pharmacol (2014), http://dx.doi.org/10.1016/j.bcp.2014.03.006

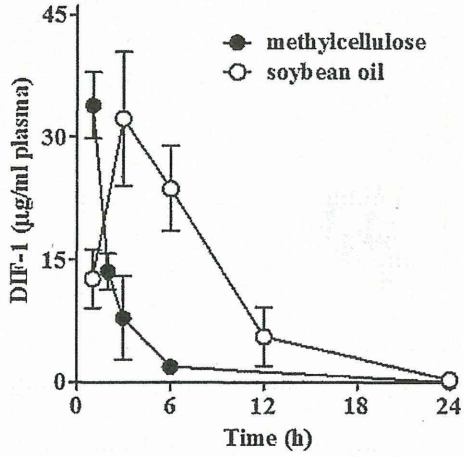

Fig. 4. Improvement of DIF-1 pharmacokinetics by dissolving it in soybean oil. Mice orally received DIF-1 suspended in methylcellulose or dissolved in soybean oil. Blood was collected at indicated times after administration and measured for plasma DIF-1 concentration using an HPLC system. $N = 3$ for each time point. Methylcellulose data (1–6 h) are the same as those shown in Fig. 1B.

observation might result from the difficulty to maintain a sufficient concentration of DIF-1 for more than 3 h (Fig. 1B).

After exploration of a method to increase DIF-1 plasma concentration, we found that soybean oil was a better solvent than methylcellulose. This effect was probably observed because of enhanced absorption, although the trough concentration at 24 h was still very low (Fig. 4). Therefore, we treated tumor-bearing nude mice with DIF-1 dissolved in soybean oil every 12 h (300 mg/kg in the morning and 150 mg/kg in the evening for 5 days/week).

As shown in Fig. 5A, DIF-1 administered in this manner significantly suppressed the growth of HCT-116-xenograft tumor masses and the tumor weight was reduced by approximately 40% compared with that of the controls. Subsequently, we found that the treatment with DIF-1 significantly decreased the phosphorylation levels of GSK-3β Ser^9 (Fig. 5B) and the protein amounts of Egr-1, TCF7L2 and cyclin D1, whereas β-catenin levels were unaltered (Fig. 5C). These results were consistent with our previous ones obtained from *in vitro* experiments using cultured HCT-116 cells, in which DIF-1 strongly inhibited HCT-116 cell proliferation by GSK-3β-mediated degradation of cyclin D1 and suppression of Egr-1 expression, which subsequently inhibited TCF7L2-mediated gene transcription without affecting β-catenin expression [27].

DIF-1 administration also significantly decreased the weight of HeLa-xenograft tumor masses (Fig. 6A). Similarly to HCT-116-xenograft tumors, the treatment with DIF-1 showed tendency to inhibit GSK-3β Ser^9 phosphorylation, although it was not statistically significant (Fig. 6B). DIF-1 treatment significantly decreased the expression of β-catenin, TCF7L2 and cyclin D1 (Fig. 6C), consistent with our previous results obtained using cultured HeLa cells [21,22], indicating that DIF-1 inhibited HeLa-xenograft tumor growth by GSK-3β-mediated degradation of cyclin D1 and suppression of the Wnt/β-catenin signaling pathway.

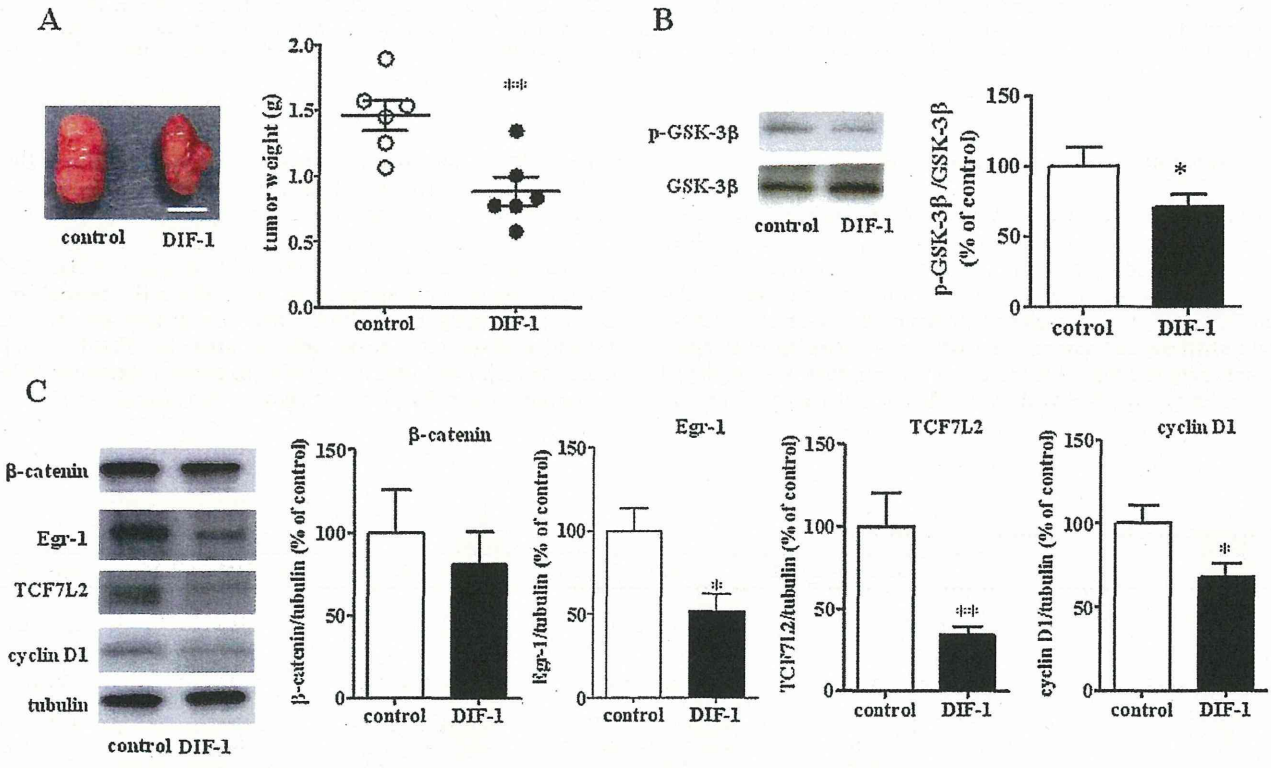

Fig. 5. Effect of orally administered DIF-1 on HCT-116-xenograft tumors.
A. Tumor appearance and weight. HCT-116 cells suspended in Matrigel were subcutaneously injected into the right flanks of mice. Tumor masses were removed after 2 weeks. Photographs show representative tumors isolated from each group of mice. Scale bar indicates 1 cm. Values are the means ± s.e.m. ($n = 6$). $^*P < 0.05$ vs. control, $^{**}P < 0.01$ vs. control (Student's *t*-test). B. GSK-3β phosphorylation levels. Protein samples were prepared from enucleated tumors and analyzed by Western blotting for phosphorylation of GSK-3β Ser^9. The membranes were stripped and then reprobed with an anti-GSK-3β antibody. Band densities are shown as percentages of the controls. Values are the means ± s.e.m. ($n = 6$). $^*P < 0.05$ vs. control (Student's *t*-test). p-GSK-3β, Ser^9 phosphorylated GSK-3β. C. Expression levels of Wnt signaling-related proteins. Protein samples were prepared from enucleated tumors and analyzed by Western blotting for β-catenin, Egr-1, TCF7L2, and cyclin D1. Band densities were quantified and normalized to those of tubulin. Values are the means ± s.e.m. ($n = 6$). $^*P < 0.05$ vs. control (Student's *t*-test).

Please cite this article in press as: Takahashi-Yanaga F, et al. DIF-1 inhibits tumor growth *in vivo* reducing phosphorylation of GSK-3β and expressions of cyclin D1 and TCF7L2 in cancer model mice. Biochem Pharmacol (2014), http://dx.doi.org/10.1016/j.bcp.2014.03.006

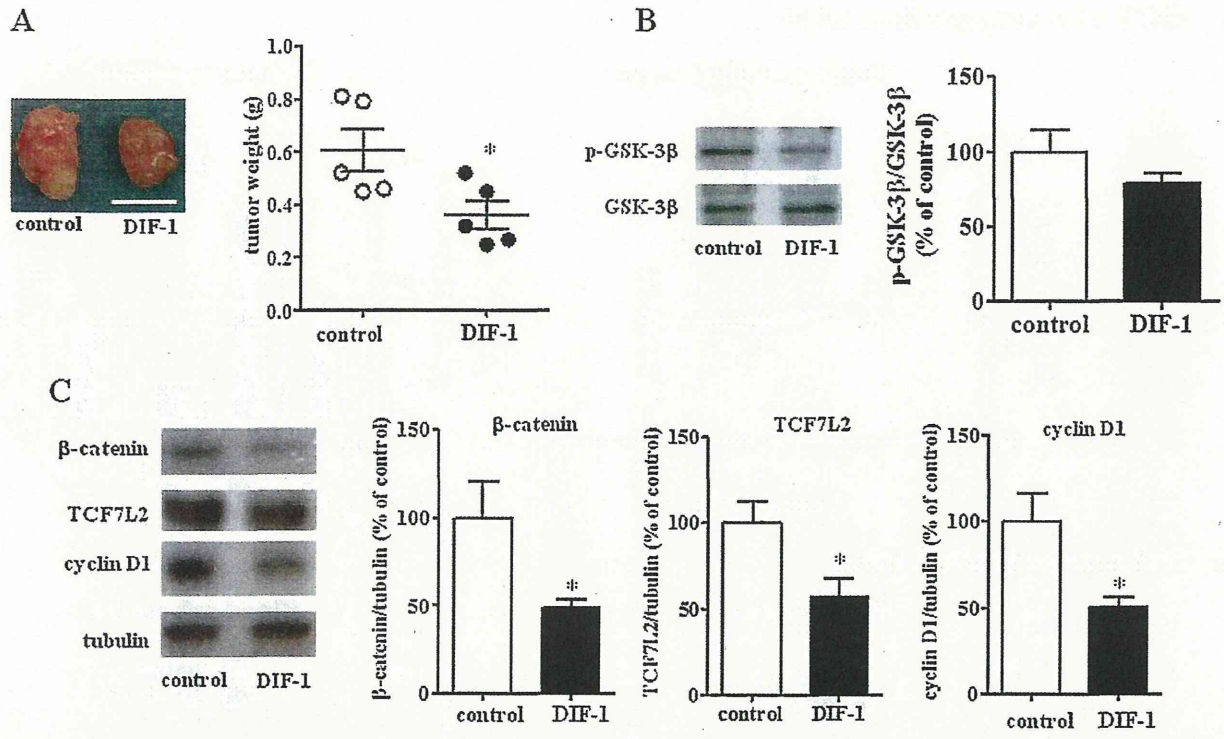

Fig. 6. Effect of orally administered DIF-1 on HeLa-xenograft tumors.
A. Tumor appearance and weight. HeLa cells suspended in Matrigel were subcutaneously injected into the right flanks of mice. Tumor masses were removed after 3 weeks. Photographs show representative tumors isolated from each group of mice. Scale bar indicates 1 cm. Values are the means ± s.e.m. ($n = 5$). *$P < 0.05$ vs. control, **$P < 0.01$ vs. control (Student's t-test). B. GSK-3β phosphorylation levels. Protein samples were prepared from enucleated tumors and analyzed by Western blotting for phosphorylation of GSK-3β Ser^9. The membranes were stripped and then reprobed with an anti-GSK-3β antibody. Band densities are shown as percentages of the controls. Values are the means ± s.e.m. ($n = 5$). *$P < 0.05$ vs. control (Student's t-test). p-GSK-3β, Ser^9 phosphorylated GSK-3β. C. Expression levels of Wnt signaling-related proteins. Protein samples were prepared from enucleated tumors and analyzed by Western blotting for β-catenin, TCF7L2, and cyclin D1. Band densities were quantified and normalized to those of tubulin. Values are the means ± s.e.m. ($n = 5$). *$P < 0.05$ vs. control (Student's t-test).

Finally, we found no significant differences in the appearance, activity, body weight, and blood cell counts between DIF-1-treated mice and the controls, despite the treatment with higher dose of DIF-1 compared with Table 1 (Fig. 7).

4. Discussion

The present study clearly showed for the first time that DIF-1 was absorbed through the digestive tract to elevate its blood concentration and inhibited *in-vivo* tumor growth without manifesting any apparent toxicity in three different cancer model animals, *Mutyh*$^{-/-}$ mice, HCT-116-bearing mice and HeLa-bearing mice, suggesting that this compound might be applicable for the treatment of human cancer. And moreover, regarding the mechanisms for the anti-tumor effect of DIF-1, we found that this compound also induced dephosphorylation of GSK-3β and reduced TCF-mediated gene transcription *in vivo*.

MUTYH is a mammalian DNA glycosylase that initiates base excision repair by excising adenine opposite 8-oxoguanine and 2-hydroxyadenine opposite guanine, thereby preventing G:C to T:A transversion mutations caused by oxidative stress [35–37]. Recently, a biallelic germline mutation of *MUTYH* has been found in humans. Those carrying this *MUTYH* mutation tend to develop multiple adenomatous colon polyps and have an increased risk of colorectal cancer in parallel with an increased incidence of G:C to T:A somatic mutations in the *APC* gene [29,30]. These mutations of the *APC* gene induce constitutive activation of Wnt/β-catenin signaling as observed in FAP patients. This type of polyposis is called MUTYH-associated polyposis (MAP). Therefore, the animal model that we employed appeared to be adequate to evaluate the clinical utility of DIF-1. The efficacy of DIF-1 for treatment of oxidative stress-induced intestinal tumors in *Mutyh*$^{-/-}$ mice was comparable with that of celecoxib, the only non-steroidal anti-inflammatory drug clinically applicable for FAP patients. Because celecoxib and DIF-1 inhibited TCF-mediated gene expression in colon cancer cells [38,39], this may be a mechanism underlying the intestinal tumor growth inhibition by DIF-1 and celecoxib.

Oral administration of DIF-1 suspended in methylcellulose inhibited tumor growth in *Mutyh*$^{-/-}$ mice, whereas at first the same treatment failed to inhibit the growth of xenograft tumors. Although we have not been able to address the precise reason for this failure, we suppose that orally administered DIF-1 might exert direct actions on tumors in the intestinal mucosa without being absorbed into systemic circulation and that the plasma concentration of DIF-1 may not have been sufficient to inhibit growth of the xenograft tumors distant from the digestive tract. It was difficult to maintain a sufficiently high plasma concentration of DIF-1 for longer than 3 h as shown in Fig. 1B. Therefore, we explored another method to improve absorption of DIF-1 and found that soybean oil was a better solvent than methylcellulose to maintain the plasma concentration of DIF-1 (Fig. 4). The reason for this may be that hydrophobic DIF-1 molecules were more soluble in oil than in water. In any case, oral administration of DIF-1 dissolved in soybean oil successfully inhibited growth of the xenograft tumors, which indicated that DIF-1 distributed through systemic circulation could inhibit tumor growth when the plasma concentration of DIF-1 was sufficiently elevated.

The phosphorylation status of GSK-3β Ser^9 indicated that DIF-1 activated or tended to activate this kinase in both *Mutyh*$^{-/-}$ mice and nude mice bearing xenograft tumors. This observation is

Please cite this article in press as: Takahashi-Yanaga F, et al. DIF-1 inhibits tumor growth *in vivo* reducing phosphorylation of GSK-3β and expressions of cyclin D1 and TCF7L2 in cancer model mice. Biochem Pharmacol (2014), http://dx.doi.org/10.1016/j.bcp.2014.03.006

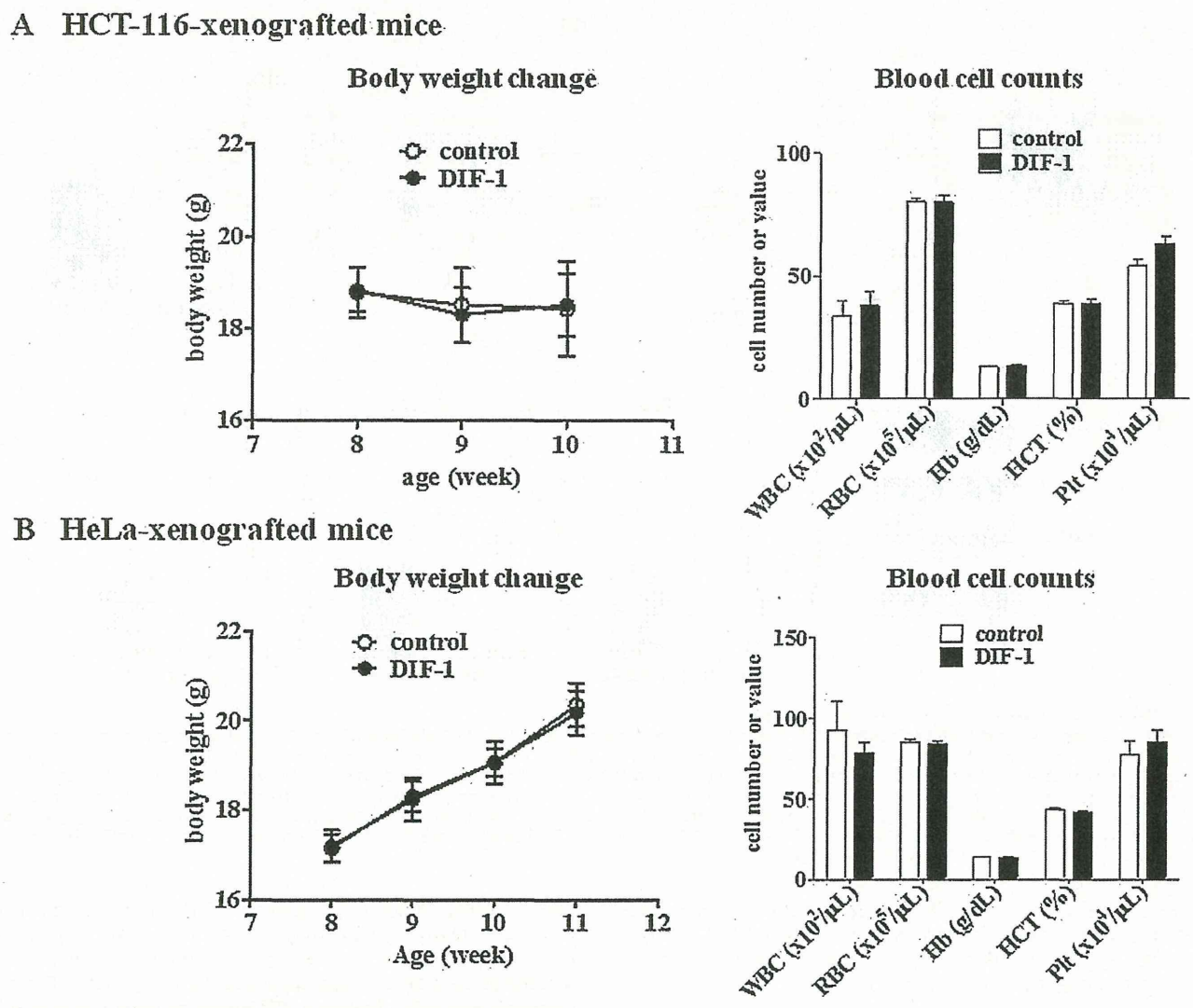

Fig. 7. Effect of DIF-1 on the body weight and blood cell counts of xenografted mice.
The body weight of xenografted mice was monitored weekly during the treatment period. Blood samples collected at the end of treatment were subjected to cell counting. A. HCT-116-xenografted mice. B. HeLa-xenografted mice. Values are the means ± s.e.m. (n = 6 for HCT-116-xenografted mice, n = 5 for HeLa-xenografted mice). WBCs, white blood cells; RBCs, red blood cells; Hb, hemoglobin; HCT, hematocrit; Plt, platelets.

consistent with our previous results obtained using cultured tumor cell lines [21–23,25,26]. Therefore, GSK-3β activiation and subsequent degradation of β-catenin may be one of important mechanisms underlying the DIF-1 action to inhibit the Wnt/β-catenin target gene expression. However, most colorectal cancers including MAP carry somatic mutations in their *APC* or *β-catenin* genes, which allow β-catenin to escape from GSK-3β-induced degradation and to accumulate in the nuclei, leading to the activation of β-catenin/TCF-mediated gene transcription [28–30]. Indeed, the β-catenin signal is constitutively activated in HCT-116 cells and probably also in the intestinal tumors developed in *Mutyh*$^{-/-}$ mice [11–14,29,30], which may be a reason why DIF-1 could not decrease β-catenin in tumors of *Mutyh*$^{-/-}$ mice and HCT-116 xenograft tumors (Figs. 3B and 5C). Despite constitutively active β-catenin, DIF-1 strongly suppressed the expression of cyclin D1 and TCF7L2 without affecting β-catenin expression levels in the intestinal tumors of *Mutyh*$^{-/-}$ mice and HCT-116-xenograft tumors. This result was consistent with our previous *in-vitro* study using HCT-116, in which we concluded that DIF-1 inhibited "Wnt target" gene expression through inhibition of Egr-1-mediated TCF7L2 gene transcription independent of β-catenin [27]. As shown in the present study, DIF-1 also suppressed the expression of Egr-1 *in vivo*, indicating that DIF-1 may inhibit tumor growth *in vivo* by the same mechanism as revealed *in vitro*.

DIF-1 may have at least three pharmaceutical merits in comparison to existing anti-cancer drugs. First, the mechanisms of its action are very unique. DIF-1 strongly inhibits the Wnt/β-catenin signaling pathway whether APC and/or β-catenin are intact or mutated, resulting in powerful suppression of the expression levels of cyclin D1 and TCF7L2. Although this pathway is often excessively activated in cancer cells, there is few anti-cancer drugs that target this pathway so far. Second, DIF-1 is unlikely to induce serious adverse reactions. DIF-1 induces cell cycle arrest at G_1 phase without affecting cell viability [21,23,25]. In the present *in-vivo* study, repeated administration of DIF-1 did not reduce the body weight or blood cell counts in mice. Certainly, it is unknown whether this cytoprotective property is advantageous in the treatment of cancer, for which cytotoxic drugs are usually used. We expect that DIF-1 is useful at least when used in combination with cytotoxic anti-cancer drugs. Third, DIF-1 can be

Please cite this article in press as: Takahashi-Yanaga F, et al. DIF-1 inhibits tumor growth *in vivo* reducing phosphorylation of GSK-3β and expressions of cyclin D1 and TCF7L2 in cancer model mice. Biochem Pharmacol (2014), http://dx.doi.org/10.1016/j.bcp.2014.03.006

applied through the digestive tract, although improvement can be required to prolong its half life in the blood. In summary, DIF-1 may have potential as a novel oral anti-cancer agent with unique mechanisms of action and less toxicity.

In addition, *in-vitro* and *in-vivo* experiments using endothelial cells have shown that DIF-1 inhibits angiogenesis by reducing the expression of vascular endothelial growth factor receptor-2, which is independent of its effect on the Wnt/β-catenin signaling pathway [26]. Therefore, inhibition of the Wnt/β-catenin signaling pathway may not be the only mechanism for the anti-tumor effect of DIF-1. Despite our efforts and those of other research groups, the target molecule(s) of DIFs for its antiproliferative effect on mammalian cells has not yet been identified [40,41]. Identification of the target molecule(s) may not only reveal the precise mechanisms for the antiproliferative effect of DIFs but also offer novel anti-cancer drugs that suppress both tumor cell proliferation and neovascularization.

Acknowledgments

We thank Issei Egashira, Naoya Kubokura, Masaki Arioka and Fumie Shiraishi (Department of Clinical Pharmacology, Faculty of Medical Sciences, Kyushu University) for technical assistance and Minako Hirahashi (Department of Anatomic Pathology, Faculty of Medical Sciences, Kyushu University) for useful discussion. This study was supported by KAKENHI to FTY (21590284 and 25460334).

References

[1] Nelson WJ, Nusse R. Convergence of Wnt, β-catenin, and cadherin pathways. Science 2004;303:1483–7.
[2] Moon RT, Bowerman B, Boutros M, Perrimon N. The promise and perils of Wnt signaling through β-catenin. Science 2002;296:1644–6.
[3] Akiyama T. Wnt/β-catenin signaling. Cytokine Growth Factor Rev 2000;11:273–82.
[4] Sherr CJ. Cancer cell cycles. Science 1996;274:1672–7.
[5] Meyer N, Penn LZ. Reflecting on 25 years with MYC. Nat Rev Cancer 2008;8:976–90.
[6] Barnes DM, Gillett CE. Cyclin D1 in breast cancer. Breast Cancer Res Treat 1998;52:1–15.
[7] Nesbit CE, Tersak JM, Prochownik EV. MYC oncogenes and human neoplastic disease. Oncogene 1999;18:3004–16.
[8] Utsunomiya T, Doki Y, Takemoto H, Shiozaki H, Yano M, Sekimoto M, et al. Correlation of β-catenin and cyclin D1 expression in colon cancers. Oncology 2001;61:226–33.
[9] Fu M, Wang C, Li Z, Sakamaki T, Pestell RG. Minireview Cyclin D1: normal and abnormal functions. Endocrinology 2004;145:5439–47.
[10] Logan CY, Nusse R. The Wnt signaling pathway in development and disease. Annu Rev Cell Dev Biol 2004;20:781–810.
[11] Morin PJ, Sparks AB, Korinek V, Barker N, Clevers H, Vogelstein B, et al. Activation of β-catenin-Tcf signaling in colon cancer by mutations in β-catenin or APC. Science 1997;275:1787–90.
[12] Satoh S, Daigo Y, Furukawa Y, Kato T, Miwa N, Nishiwaki T, et al. AXIN1 mutations in hepatocellular carcinomas, and growth suppression in cancer cells by virus-mediated transfer of AXIN1. Nat Genet 2000;24:245–50.
[13] McDonald SA, Preston SL, Lovell MJ, Wright NA, Jankowski JA. Mechanisms of disease: from stem cells to colorectal cancer. Nat Clin Pract Gastroenterol Hepatol 2006;3:267–74.
[14] Segditsas S, Tomlinson I. Colorectal cancer and genetic alterations in the Wnt pathway. Oncogene 2006;25:7531–7.
[15] Cohen P, Frame S. The renaissance of GSK3. Nat Rev Mol Cell Biol 2001;2:769–76.
[16] Frame S, Cohen P. GSK3 takes centre stage more than 20 years after its discovery. Biochem J 2001;359:1–16.
[17] Diehl JA, Cheng M, Roussel MF, Sherr CJ. Glycogen synthase kinase-3β regulates cyclin D1 proteolysis and subcellular localization. Genes Dev 1998;12:3499–511.
[18] Takahashi-Yanaga F, Sasaguri T. GSK-3β regulates cyclin D1 expression: a new target for chemotherapy. Cell Signal 2008;20:581–9.
[19] Morris HR, Taylor GW, Masento MS, Jermyn KA, Kay RR. Chemical structure of the morphogen differentiation inducing factor from *Dictyostelium discoideum*. Nature 1987;328:811–4.
[20] Morris HR, Masento MS, Taylor GW, Jermyn KA, Kay RR. Structure elucidation of two differentiation inducing factors (DIF-2 and DIF-3) from the cellular slime mould *Dictyostelium discoideum*. Biochem J 1988;249:903–6.
[21] Takahashi-Yanaga F, Taba Y, Miwa Y, Kubohara Y, Watanabe Y, Hirata M, et al. Dictyostelium differentiation-inducing factor-3 activates glycogen synthase kinase-3β and degrades cyclin D1 in mammalian cells. J Biol Chem 2003;278:9663–70.
[22] Yasmin T, Takahashi-Yanaga F, Mori J, Miwa Y, Hirata M, Watanabe Y, et al. Differentiation-inducing factor-1 suppresses gene expression of cyclin D1 in tumor cells. Biochem Biophys Res Commun 2005;338:903–9.
[23] Mori J, Takahashi-Yanaga F, Miwa Y, Watanabe Y, Hirata M, Morimoto S, et al. Differentiation-inducing factor-1 induces cyclin D1 degradation through the phosphorylation of Thr^{286} in squamous cell carcinoma. Exp Cell Res 2005;310:426–33.
[24] Takahashi-Yanaga F, Mori J, Matsuzaki E, Watanabe Y, Hirata M, Miwa Y, et al. Involvement of GSK-3β and DYRK1B in differentiation-inducing factor-3-induced phosphorylation of cyclin D1 in HeLa cells. J Biol Chem 2006;281:38489–97.
[25] Matsuzaki E, Takahashi-Yanaga F, Miwa Y, Hirata M, Watanabe Y, Sato N, et al. Differentiation-inducing factor-1 alters canonical Wnt signaling and suppresses alkaline phosphatase expression in osteoblast-like cell lines. J Bone Miner Res 2006;21:1307–16.
[26] Yoshihara T, Takahashi-Yanaga F, Shiraishi F, Morimoto S, Watanabe Y, Hirata M, et al. Anti-angiogenic effects of differentiation-inducing factor-1 involving VEGFR-2 expression inhibition independent of the Wnt/β-catenin signaling pathway. Mol Cancer 2010;9:245.
[27] Jingushi K, Takahashi-Yanaga F, Yoshihara T, Shiraishi F, Watanabe Y, Hirata M, et al. DIF-1 inhibits the Wnt/β-catenin signaling pathway by inhibiting TCF7L2 expression in colon cancer cell lines. Biochem Pharmacol 2012;83:47–56.
[28] Al-Tassan N, Chmiel NH, Maynard J, Fleming N, Livingston AL, Williams GT, et al. Inherited variants of MYH associated with somatic G:C–>T:A mutations in colorectal tumors. Nat Genet 2002;30:227–32.
[29] Sampson JR, Dolwani S, Jones S, Eccles D, Ellis A, Evans DG, et al. Autosomal recessive colorectal adenomatous polyposis due to inherited mutations of MYH. Lancet 2003;362:39–41.
[30] Sieber OM, Lipton L, Crabtree M, Heinimann K, Fidalgo P, Phillips RK, et al. Multiple colorectal adenomas, classic adenomatous polyposis, and germ-line mutations in MYH. N Engl J Med 2003;348:791–9.
[31] Sakamoto K, Tominaga Y, Yamauchi K, Nakatsu Y, Sakumi K, Yoshiyama K, et al. MUTYH-null mice are susceptible to spontaneous and oxidative stress induced intestinal tumorigenesis. Cancer Res 2007;67:6599–604.
[32] Masento MS, Morris HR, Taylor GW, Johnson SJ, Skapski AC, Kay RR. Differentiation-inducing factor from the slime mould *Dictyostelium discoideum* and its analogues. Synthesis, structure and biological activity. Biochem J 1988;256:23–8.
[33] Traynor D, Kay RR. The DIF-1 signaling system in Dictyostelium. Metabolism of the signal. J Biol Chem 1991;266:5291–7.
[34] Steinbach G, Lynch PM, Phillips RK, Wallace MH, Hawk E, Gordon GB, et al. The effect of celecoxib, a cyclooxygenase-2 inhibitor, in familial adenomatous polyposis. N Engl J Med 2000;342:1946–52.
[35] Ohtsubo T, Nishioka K, Imaiso Y, Iwai S, Shimokawa H, Oda H, et al. Identification of human MutY homolog (hMYH) as a repair enzyme for 2-hydroxyadenine in DNA and detection of multiple forms of hMYH located in nuclei and mitochondria. Nucleic Acids Res 2000;28:1355–64.
[36] Hirano S, Tominaga Y, Ichinoe A, Ushijima Y, Tsuchimoto D, Honda-Ohnishi Y, et al. Mutator phenotype of MUTYH-null mouse embryonic stem cells. J Biol Chem 2003;278:38121–24.
[37] Klungland A, Rosewell I, Hollenbach S, Larsen E, Daly G, Epe B, et al. Accumulation of premutagenic DNA lesions in mice defective in removal of oxidative base damage. Proc Natl Acad Sci USA 1999;96:13300–05.
[38] Sakoguchi-Okada N, Takahashi-Yanaga F, Fukada K, Shiraishi F, Taba Y, Miwa Y, et al. Celecoxib inhibits the expression of survivin via the suppression of promoter activity in human colon cancer cells. Biochem Pharmacol 2007;73:1318–29.
[39] Takahashi-Yanaga F, Yoshihara T, Jingushi K, Miwa Y, Morimoto S, Hirata M, et al. Celecoxib-induced degradation of T-cell factors-1 and -4 in human colon cancer cells. Biochem Biophys Res Commun 2008;377:1185–90.
[40] Matsuda T, Takahashi-Yanaga F, Yoshihara T, Maenaka K, Watanabe Y, Miwa Y, et al. Dictyostelium differentiation-inducing factor-1 binds to mitochondrial malate dehydrogenase and inhibits its activity. J Pharmacol Sci 2010;112:320–6.
[41] Shimizu K, Murata T, Tagawa T, Takahashi K, Ishikawa R, Abe Y, et al. Calmodulin-dependent cyclic nucleotide phosphodiesterase (PDE1) is a pharmacological target of differentiation-inducing factor-1, an antitumor agent isolated from Dictyostelium. Cancer Res 2004;64:2568–71.

Please cite this article in press as: Takahashi-Yanaga F, et al. DIF-1 inhibits tumor growth *in vivo* reducing phosphorylation of GSK-3β and expressions of cyclin D1 and TCF7L2 in cancer model mice. Biochem Pharmacol (2014), http://dx.doi.org/10.1016/j.bcp.2014.03.006

IVYSPRING INTERNATIONAL PUBLISHER

International Journal of Biological Sciences

2014; 10(1):73-79. doi: 10.7150/ijbs.5750

Research Paper

Mismatch Repair Deficient Mice Show Susceptibility to Oxidative Stress-Induced Intestinal Carcinogenesis

Jingshu Piao[1], Yoshimichi Nakatsu[1], Mizuki Ohno[1], Ken-ichi Taguchi[2], Teruhisa Tsuzuki[1] ✉

1. Department of Medical Biophysics and Radiation Biology, Graduate School of Medical Sciences, Kyushu University,
2. Department of Cancer Pathology, Institute for Clinical Research, National Kyushu Cancer Center, Fukuoka, Japan

✉ Corresponding author: Teruhisa Tsuzuki, Department of Medical Biophysics and Radiation Biology, Faculty of Medical Sciences, Kyushu University, Fukuoka 812-8582, Japan. Phone: +81-92-642-6141: fax: +81-92-642-6145: E-mail: tsuzuki@med.kyushu-u.ac.jp

Received: 2012.12.21; Accepted: 2013.07.24; Published: 2013.12.19

Abstract

We have previously established an experimental system for oxidative DNA damage-induced tumorigenesis in the small intestine of mice. To elucidate the roles of mismatch repair genes in the tumor suppression, we performed oxidative DNA damage-induced tumorigenesis experiments using *Msh2*-deficient mice. Oral administration of 0.2% Potassium Bromate, $KBrO_3$, effectively induced epithelial tumors in the small intestines of *Msh2*-deficient mice. We observed a 22.5-fold increase in tumor formation in the small intestines of *Msh2*-deficient mice compared with the wild type mice. These results indicate that mismatch repair is involved in the suppression of oxidative stress-induced intestinal tumorigenesis in mice. A mutation analysis of the *Ctnnb1* gene of the tumors revealed predominant occurrences of G:C to A:T transitions. The TUNEL analysis showed a decreased number of TUNEL-positive cells in the crypts of small intestines from the *Msh2*-deficient mice compared with the wild type mice after treatment of $KBrO_3$. These results suggest that the mismatch repair system may simultaneously function in both avoiding mutagenesis and inducing cell death to suppress the tumorigenesis induced by oxidative stress in the small intestine of mice.

Key words: HNPCC, oxidative DNA damage, Wnt signaling pathway, mutagenesis, cell death

Introduction

Reactive oxygen species (ROS) are generated by the normal cellular metabolism and also by exposure to environmental factors, such as radiation and chemicals. ROS constantly induce various lesions in the DNA of living organisms under physiological conditions, and the resulting DNA damage causes mutations and cell death, leading to aging-associated diseases, such as cancer and neurodegeneration (1). Among the various types of oxidative DNA damage, oxidized guanine, 8-oxo-7, 8-dihydroguanine (8-oxoG) is abundant and highly mutagenic because of its ambiguous base-pairing properties; it can be paired with adenine as well as with cytosine (2-6). Therefore, 8-oxoG in DNA causes G:C to T:A transversions after two rounds of DNA replication. In mammalian cells, the base excision repair (BER) pathway initiated by OGG1 or MUTYH plays a role in the suppression of 8-oxoG-related mutagenesis. OGG1, an 8-oxoG DNA glycosylase, excises the 8-oxoG paired with cytosine from DNA (7, 8). MUTYH is an adenine DNA glycosylase that excises the adenine incorporated opposite 8-oxoG from DNA (9-12). The synergistic actions of OGG1 and MUTYH suppress the mutagenesis caused by 8-oxoG in DNA.

In addition to DNA repair, a nucleotide pool sanitizing enzyme, MTH1, suppresses the mutagenesis induced by oxidative stress (13, 14). This enzyme can hydrolyze oxidized purine nucleotides, such as 8-oxo-dGTP, 2-OH-dATP and 8-OH-dATP, to prevent the incorporation of mutagenic nucleotides into DNA

during replication (15, 16). In addition to 8-oxoG, a wide variety of oxidatively modified bases in DNA were removed by the BER pathway following initiation by various DNA glycosylases (17).

Besides BER, mismatch repair (MMR) is also involved in the repair of oxidative DNA damage. MMR is an evolutionarily conserved system that corrects replication errors such as mismatched bases and small insertions/deletions. The MSH2/MSH6 heterodimer (MutSα) and MSH2/MSH3 heterodimer (MutSβ) recognize mismatched bases and small insertions/deletions, respectively, and then recruit MutLα (MLH1 and PMS2 heterodimer) to initiate the MMR reaction (18). In addition to its role in correcting replication errors, MMR is known to involve in the induction of apoptosis in response to DNA lesions caused by alkylating agents (19-21). The human MMR genes are associated with hereditary non-polyposis colorectal cancer (HNPCC), which is a common cancer predisposition syndrome characterized by a dominant mode of transmission and high penetrance (22-25). deWeese *et al* reported that *Msh2*-deficient mouse embryonic stem (ES) cells showed the accumulation of oxidative DNA damage, such as 8-oxoG and thymine glycol, in their genomes, as well as tolerance to apoptosis caused by low dose gamma-ray irradiation (26). Based on the analysis of spontaneous mutational specificity of mice defective in the *Mth1* and/or the *Msh2* genes, we speculated that MMR might act to correct mispairs with the oxidized nucleotides (27). Furthermore, Colussi *et al*, and Russo *et al* reported that MMR could suppress the mutations caused by the incorporation of oxidized purine deoxynucleoside triphosphate (28, 29). These findings suggest the involvement of MMR in the suppression of oxidative stress-induced mutagenesis and tumorigenesis in mammals.

$KBrO_3$ is an oxidizing agent that is known to induce 8-oxoG in the DNA of rats and mice, and is recognized as a renal carcinogen in rats (30-33). We previously established an experimental system for oxidative DNA damage-induced tumorigenesis in the intestinal tract of mice using this agent (34). The oral administration of $KBrO_3$ for 16 weeks effectively induced epithelial tumors in the small intestines of *Mutyh*-deficient mice, indicating the significance of Mutyh in the suppression of tumorigenesis induced by oxidative stress (34).

In this study, we performed $KBrO_3$-induced tumorigenesis experiments using *Msh2*-deficient mice to elucidate the roles of MMR in the suppression of oxidative stress-induced tumorigenesis. We found that MMR plays a significant role in the suppression of oxidative stress-induced intestinal tumorigenesis in mice.

Materials and Methods

Animals

The *Msh2*-deficient mice used in this study were generated as reported previously (27). The wild type, heterozygous and homozygous mutant mice used in this study were obtained by intercrossing the heterozygous mutant mice. All animals were maintained under specific pathogen free (SPF) conditions. All animal care and handling procedures were approved by the Institutional Animal Care and Use Committee of Kyushu University, and followed the Guideline for Proper Conduct of Animal Experiments, Science Council of Japan.

$KBrO_3$ treatment

$KBrO_3$ (Sigma-ALDRICH) was given to 6~8-week-old mice in their drinking water at a concentration of 0.2% for 16 weeks. The body weight and consumption of drinking water were measured every week. After 16 weeks, all the animals were sacrificed, and the intestines were fixed with 10% phosphate buffered-formalin, and then stored in 70% ethanol.

Histological analysis

The inspections for tumor formation in the intestinal mucosa were carefully performed under a dissecting microscope. The small intestinal tumors were carefully removed from intestines, embedded in paraffin and sectioned. The sections were stained with hematoxylin and eosin for the diagnosis of the tumors. The evaluation of the tumors was performed according to the Vienna classification (35).

Mutation analysis of the *Ctnnb1* gene

The small intestinal tumors were carefully removed from the mucosa under a dissecting microscope. Genomic DNA was extracted using a DNeasy Tissue Kit (QIAGEN) according to the manufacturer's protocol. Eighty-nine small intestinal tumors obtained from five *Msh2*-deficient mice were analyzed for mutations in the *Ctnnb1* (*β-catenin*) gene. Thirty to fifty nanograms of genomic DNA extracted from each small intestinal tumor was used as the template for PCR with rTaq DNA polymerase (TaKaRa). The entire coding sequence of the second exon of the *Ctnnb1* gene was amplified using primers 5′-TCCTTGGCTGCCTTTCTAACAGTA-3′ (upper) and 5′-GCATGCCCTCATCTAGCGTCT-3′ (lower). Amplified DNA containing exon 2 of the *Ctnnb1* gene was purified with a PCR purification kit (QIAGEN) according to the manufacturer's protocol. The purified DNA fragments were used as a template for direct sequencing with a BigDye Terminator v3.1 Cycle Sequencing kit (Applied Biosystems) and the se-

quences were determined with an ABI PRISM® 3100 Genetic Analyzer (Applied Biosystems).

TUNEL analysis

The intestines were removed from the wild type and mutant mice treated with $KBrO_3$ for 16 weeks, and 3 μm sections were made after the samples were embedded in paraffin. We analyzed the cell death (apoptosis) in the crypts of the small intestine using a TUNEL kit (TaKaRa) as described in the manual supplied by the manufacturer. We counted the TUNEL-positive cells in more than 100 crypts from five mice of each genotype.

Results

Tumor formation induced by $KBrO_3$ treatment in *Msh2*-deficient mice

In order to examine whether oxidative stress increases the intestinal tumorigenesis in mismatch repair-deficient mice, congenic wild type, heterozygous and homozygous *Msh2*-deficient (5, 6 and 7 animals for each genotype, respectively) mice were administered 0.2% $KBrO_3$ in their drinking water for 16 weeks. At the same time, five mice of each genotype were kept under the same conditions except for the $KBrO_3$-treatment. As previously observed, the $KBrO_3$-treatment appeared to cause a slowdown in the increase of body weight at almost the same rate in all groups of animals during the period of $KBrO_3$-treatment. We dissected the mice after the 16-week treatment with $KBrO_3$, and inspected the intestines under a dissecting microscope. In the homozygous *Msh2*-deficient mice treated with $KBrO_3$, the formation of small intestinal tumors was dramatically increased (Figure 1, Table 1). The mean number of tumors induced in the small intestines of the seven *Msh2*-deficient mice was 27.0, whereas it was 1.2 and 1.5 in the five wild type and six heterozygous mice, respectively. Tumor formation was also observed in the untreated homozygous *Msh2*-deficient mice, albeit at a much lower frequency (mean: 1.2 tumor/mouse, n=5) compared with the treated homozygous mice. As previously observed in the *Mutyh*-deficient mice (34), the $KBrO_3$-induced tumors predominantly developed in the duodenum and in the upper region of the jejunum (Figure 1A). We found no other anomalies in the $KBrO_3$-treatment mice.

Table 1. Tumor formation in the intestine of *Msh2*-deficient mice

Genotype	No treatment	$KBrO_3$-treatment	
	No. of tumors[a]	No. of tumors[a]	Ratio[b]
Wild type	0	1.20 ± 0.98	1.00
Heterozygote	0	1.50 ± 1.26	1.25
Homozygote	1.20 ± 0.75	27.00 ± 7.44	22.50

a: The no. of tumors is the mean number of tumors per mouse, with the standard deviation. b: ratio to tumors in wild type mice

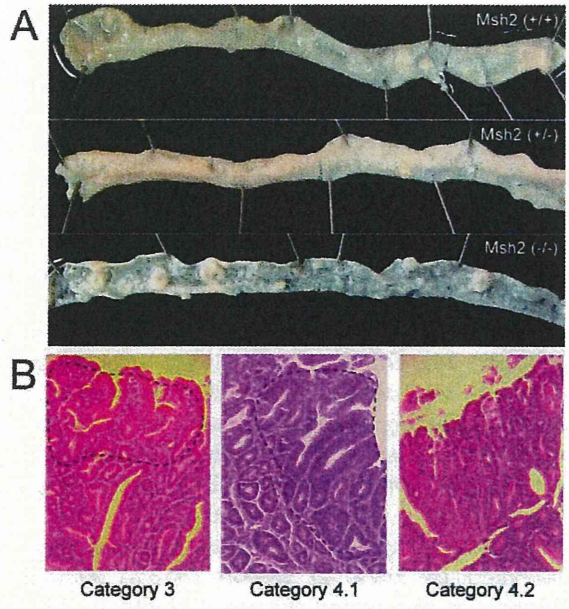

Figure 1. $KBrO_3$-induced tumors in the small intestine of *Msh2*-deficient mice. A. The proximal regions of the small intestines of $KBrO_3$-treated mice are shown; (+/+): wild type, (+/-): heterozygous *Msh2*-deficient, and (-/-): homozygous *Msh2*-deficient mice. Multiple polyp formations could be observed in the $KBrO_3$-treated homozygous *Msh2*-deficient mice. **B.** A section of a $KBrO_3$-induced tumor stained with hematoxylin and eosin (original magnification: objective 10X). The regions containing the neoplasia are encircled by a broken line.

Pathological analysis of tumors induced by $KBrO_3$ in the small intestines

We performed a pathological analysis of 25, three and two small intestinal tumors derived from five homozygous-deficient, three heterozygous *Msh2*-deficient mice and two wild type mice, respectively, according to the Vienna classification of gastrointestinal epithelial neoplasia (Table 2, Figure 1B). All tumors from homozygous *Msh2*-deficient mice were classified as category 4 (non-invasive high grade neoplasia), except for one case that was classified as category 3 (non-invasive low grade neoplasia). All tumors from wild type and heterozygous *Msh2*-deficient mice were also classified as category 4 (Table 2).

Table 2. Classification of $KBrO_3$-induced small intestinal tumors in mice

Genotype	Category 3*	Category 4*			Total
		4.1	4.2	4.3	
Wild type	—	—	2	—	2
Heterozygote	—	—	3	—	3
Homozygote	1	3	21	—	25

*Tumors were categorized according to the Vienna classification of gastrointestinal epithelial neoplasia

Mutation analysis of the *Ctnnb1* gene

The β-catenin protein encoded by *Ctnnb1* gene is a transcriptional activator functioning in the Wnt-signaling pathway (36). The phosphorylation of β-catenin by GSK3β in a complex with Axin and Apc is required for the ubiquitin-mediated degradation of β-catenin. Therefore, the presence of mutations affecting the phosphorylation of the protein lead to its stabilization and the accumulation of β-catenin in nuclei, inducing the expression of target genes such as c-myc and cyclin D1 without Wnt signaling. The mutations at four putative GSK3β-phosphorylation sites (S33, S37, T41, S45) and amino acids adjacent these sites have been detected in a wide variety of human cancers including HNPCC, as well as in chemically-induced tumors in model animals. Therefore, we analyzed the mutations in exon 2 of the *Ctnnb1* gene encoding the GSK3β-phosphorylation sites of β-catenin. Among 89 tumors from five homozygous *Msh2*-deficient mice, 27 tumors (30.3%) showed a mutation in this region (Figure 2, Table 3). All the mutations were base substitutions and occurred at or in the vicinity of the codons for S33, S37 and T41. No mutations were observed at the codon for S45. Among them, G:C to A:T transitions predominantly occurred; 20 mutations (74.1%) were identified as G:C to A:T transitions, and the others were three A:T to G:C transitions (11.1%), two G:C to T:A transversions and two G:C to C:G transversions (7.4%, respectively). There is no clear hotspot for G:C to A:T transitions in this region, with there being seven at D32, five at S37, four at G34 and four at T41. However, besides one G:C to T:A transversion at S33, three other types of mutations were observed only at the codon for S37. The base substitutions observed at the codon for S37 were as follows; five G:C to A:T transitions, three A:T to G:C transitions, two G:C to C:G transversions and one G:C to T:A transversion.

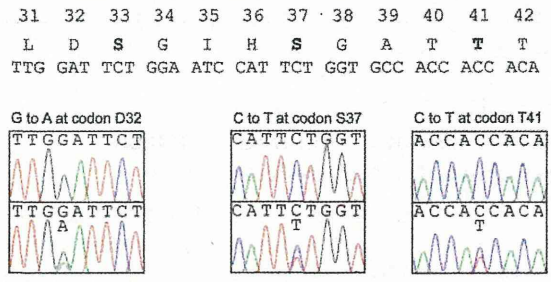

Figure 2. Somatic mutations found in the *Ctnnb1* gene of tumors. The amino acid sequence and the corresponding nucleotide sequence of GSK3β phosphorylation sites are shown at the top. The amino acids at phosphorylation sites are depicted in bold. The somatic mutations found in the $KBrO_3$-induced intestinal tumors are shown below the nucleotide sequence of the *Ctnnb1* gene; upper and lower panels show the nucleotide sequencing results from normal tissues and tumors, respectively.

Table 3. Mutations found in the *Ctnnb1* gene

Mouse ID	Sample ID	Nucleotide position	Wild type	Mutant	Mutation	Amino acid change
22	1	94	GAT	AAT	G:C→A:T	D32N
38	1	109	TCT	CCT	A:T→G:C	S37P
	4	109	TCT	CCT	A:T→G:C	S37P
	5	122	ACC	ATC	G:C→A:T	T41I
	7	101	GGA	GAA	G:C→A:T	G34E
	8	110	TCT	TAT	G:C→T:A	S37Y
	12	94	GAT	AAT	G:C→A:T	D32N
	13	100	GGA	AGA	G:C→A:T	G34R
	18	110	TCT	TTT	G:C→A:T	S37F
	20	110	TCT	TTT	G:C→A:T	S37F
	21	122	ACC	ATC	G:C→A:T	T41I
	22	94	GAT	AAT	G:C→A:T	D32N
48	4	110	TCT	TGT	G:C→C:G	S37C
	6	110	TCT	TTT	G:C→A:T	S37F
	10	94	GAT	AAT	G:C→A:T	D32N
	15	100	GGA	AGA	G:C→A:T	G34R
	22	109	TCT	CCT	A:T→G:C	S37P
45	1	122	ACC	ATC	G:C→A:T	T41I
	3	110	TCT	TGT	G:C→C:G	S37C
	9	110	TCT	TTT	G:C→A:T	S37F
	10	94	GAT	AAT	G:C→A:T	D32N
50	5	122	ACC	ATC	G:C→A:T	T41I
	8	100	GGA	AGA	G:C→A:T	G34R
	12	94	GAT	AAT	G:C→A:T	D32N
	14	94	GAT	AAT	G:C→A:T	D32N
	16	110	TCT	TTT	G:C→A:T	S37F
	24	98	TCT	TAT	G:C→T:A	S33Y